# Laser-Induced Solid-Phase Doped Graphene

**Insung Choi,[†] Hu Young Jeong,[§] Dae Yool Jung,[‡] Myunghwan Byun,[†] Choon-Gi Choi,[∥] Byung Hee Hong,[⊥] Sung-Yool Choi,[‡,*] and Keon Jae Lee[†,*]**

[†]Department of Materials Science and Engineering and [‡]Department of Electrical Engineering and Graphene Research Center, Korea Advanced Institute of Science and Technology (KAIST), Daejeon 305-701, Republic of Korea, [§]UNIST Central Research Facilities (UCRF) and School of Mechanical and Advanced Materials Engineering, Ulsan National Institute of Science and Technology (UNIST), Ulsan 689-798, Republic of Korea, [∥]Creative Research Center for Graphene Electronics, Electronics and Telecommunications Research Institute (ETRI), Daejeon 305-700, Republic of Korea, and [⊥]Department of Chemistry, Seoul National University, Seoul 151-747, Republic of Korea

**ABSTRACT** There have been numerous efforts to improve the performance of graphene-based electronic devices by chemical doping. Most studies have focused on gas-phase doping with chemical vapor deposition. However, that requires a complicated transfer process that causes undesired doping and defects by residual polymers. Here, we report a solid-phase synthesis of doped graphene by means of silicon carbide (SiC) substrate including a dopant source driven by pulsed laser irradiation. This method provides *in situ* direct growth of doped graphene on an insulating SiC substrate without a transfer step. A numerical simulation on the temperature history of the SiC surface during laser irradiation reveals that the surface temperature of SiC can be accurately controlled to grow nitrogen-doped graphene from the thermal decomposition of nitrogen-doped SiC. Laser-induced solid-phase doped graphene is highly promising for the realization of graphene-based nanoelectronics with desired functionalities.

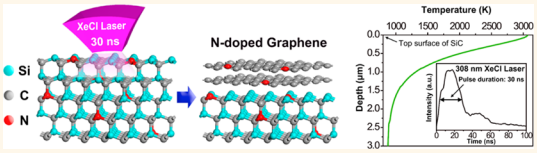


**KEYWORDS:** solid-phase synthesis · nitrogen-doped graphene · laser · silicon carbide

Graphene, a monolayer of carbon atoms arranged to form a two-dimensional honeycomb lattice, has unique physical properties such as an ambipolar electric field effect, anomalous quantum hall effect, and massless relativistic carriers.[1,2] In addition, because of its high mobility of charge carriers (200000 $cm^2\ V^{-1}\ s^{-1}$), graphene-based electronic devices have been considered promising candidates for postsilicon electronics.[3−5] In order to construct logic circuits based on graphene field effect transistors, it is inevitably desirable to realize both p-type and n-type conduction of graphene channels. The chemical doping of heterogeneous atoms into the graphene lattice could be an effective approach to tailor the electronic properties of graphene.[6,7]

Both theoretical and experimental investigations have revealed that the chemical properties of doped graphene can considerably change its physical and chemical properties, such as dopant density and bonding conformation.[8−10] Many research groups have been synthesizing and characterizing doped graphene using chemical vapor deposition (CVD);[8−12] however, this method requires a complicated transfer process,[13−15] which inevitably leads to undesired doping and defects. Alternative methods to synthesize doped epitaxial graphene (EG) by supplying nitrogen gas and ion implantation were reported, providing direct growth of doped graphene on an insulating substrate without any additional transfer procedure.[16−19] However, the extremely high temperature process (~2000 K) in the furnace limits its compatibility with industrial semiconductor applications. Therefore, a simple and robust doping methodology to realize graphene-based electronic devices with excellent reliability and performance is highly desirable.

Herein, we introduce a synthesis method of laser-induced solid-phase doped graphene using SiC substrate including a solid dopant source. Laser-induced graphene by localized heating has been recently reported using excimer laser technology,[20,21] which is widely commercialized in GaN lift-off[22] and low temperature polycrystalline silicon (LTPS).[23] The novel synthesis of solid-phase doped graphene by laser irradiation provides *in situ* direct growth of doped graphene on an insulating substrate without a complicated transfer process. Solid-phase

* Address correspondence to keonlee@kaist.ac.kr, sungyool.choi@kaist.ac.kr.

Received for review December 9, 2013 and accepted July 9, 2014.

**Published online July 09, 2014**
**10.1021/nn5032214**

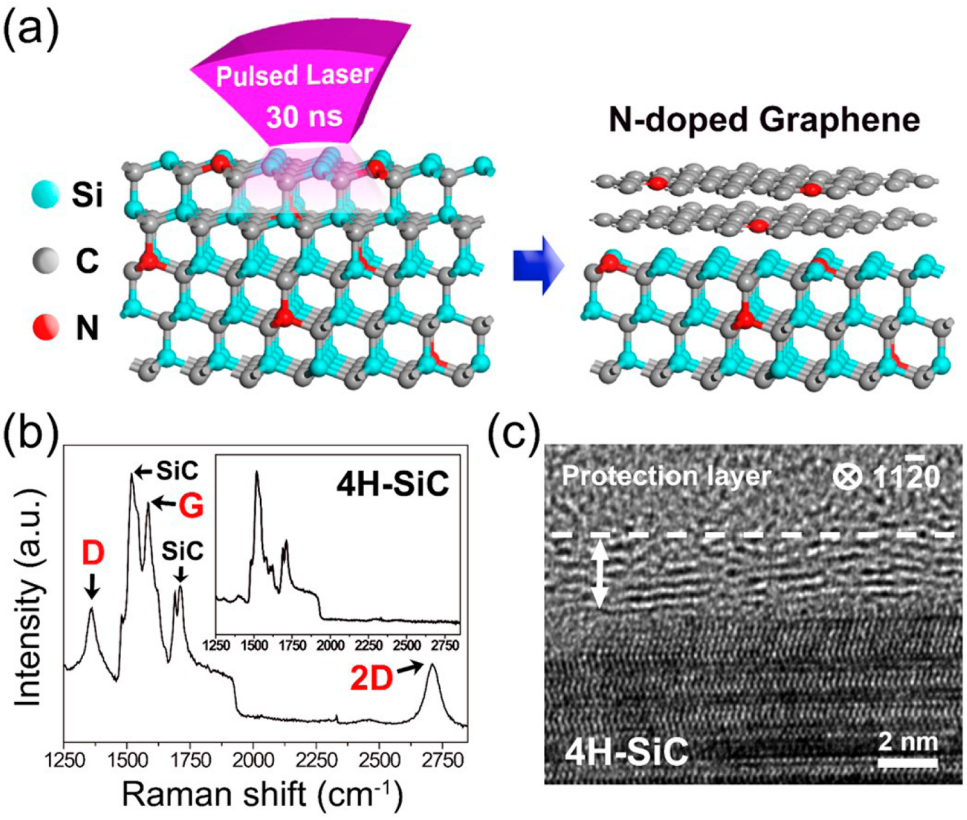


**Figure 1. (a) Schematic illustration of the synthesis method for laser-induced N-doped graphene on N-doped SiC substrate. The binding of Si−N−C was decomposed by laser irradiation, and Si atoms on the SiC surface were simultaneously evaporated to form nitrogen-doped graphene. (b) Raman spectra obtained from multilayer N-doped graphene grown on 4H-SiC. The indexed sharp spectra agree well with the D, G, and 2D band of graphene. The inset shows the characteristic of 4H-SiC substrate. (c) Cross-sectional HRTEM image of multilayer N-doped graphene on 4H-SiC (0001).**

doping can provide precise controllability of doping concentration compared with gas-phase doped graphene. We successfully synthesized nitrogen-doped graphene (N-doped graphene) on an N-doped SiC substrate and characterized it by Raman, high-resolution transmission electron microscopy (HRTEM), and X-ray photoelectron spectroscopy (XPS). In addition, a numerical simulation was performed to understand thermal behavior on the SiC surface during laser irradiation (30 ns).[24−27] Our simulation results, based on optimized experimental conditions, show that the growth temperature of laser-induced graphene is similar to the melting temperature of SiC (3100 K).[27,28] This indicates that a higher thermal energy is required to decompose Si−C bonds, compared with the classical thermal decomposition of SiC.[29−31] Through systematic analysis of the G band shift in Raman spectra,[32−34] it was confirmed that the doping concentration of the graphene can be readily controlled by changing the dopant concentration of the SiC substrate. The obtained results demonstrate that the solid dopant source of the SiC substrate could be incorporated into the graphene lattice by laser irradiation, which may open up the potential for designing solid-phase doping to realize graphene-based nanoelectronics.

## RESULTS AND DISCUSSION

Figure 1a describes a schematic of the synthesis method for N-doped graphene on N-doped SiC by pulsed laser irradiation. Hexagonal SiC materials have a wide bandgap of ~3.2 eV and thermal conductivity of 490 W/m·K.[35] Therefore, ultraviolet (UV) wavelength and high energy density are required to generate heat on the SiC surface through the light absorption process. A XeCl ($\lambda$ = 308 nm, pulse duration ~30 ns) excimer laser system with beam homogenizer and 8× projection lens was utilized to focus the UV light beam on the SiC specimen through a shadow mask patterned with a square hole (see the Supporting Information for details of laser system, Figure S1). To avoid a reaction with oxygen, the laser irradiation was performed in a vacuum condition (~$1 \times 10^{-6}$ Torr) with average fluence (*i.e.*, laser energy per unit area) of 1124 mJ/cm$^2$. We confirmed that 600 pulses (10 Hz, 60 s) were needed to evaporate Si atoms for the formation of graphene on the SiC, owing to the short pulse duration of 30 ns (Figure S2 in the Supporting Information).[20,21]

Raman spectroscopy has been widely used as a powerful and nondestructive technique to characterize the structure and electronic properties of carbon-based materials.[36,37] Figure 1b shows a Raman spectrum of N-doped graphene grown on a N-doped

4H-SiC with dopant concentration, $n = 2.2 \times 10^{18}$ cm$^{-3}$. Three representative bands, including the defect-induced D band, in-plain vibrational G band, and two-phonon scattered 2D band, are clearly observed at 1361, 1584, and 2709 cm$^{-1}$, respectively.[16,37,38] The 2D band of the multilayer N-doped graphene grown on Si-terminated surface by laser irradiation was fitted with single Lorentzian having a the full width at half-maximum (fwhm) of ~60 cm$^{-1}$, in agreement with the previous report.[20] The inset of Figure 1b represents the Raman spectrum of the 4H-SiC substrate showing characteristic peaks at 1518 and 1711 cm$^{-1}$. For more clearly investigating crystallographic features of the multilayer N-doped graphene grown on the 4H-SiC, high-resolution transmission electron microscopy (HRTEM) analysis was performed. Figure 1c shows the multilayer (4 to 5) graphene with some defective regions observed along the [11$\bar{2}$0] SiC zone axis. The average interlayer distance is about 0.38 nm between graphene layers.

Figure 2a compares the C 1s XPS spectra of pristine (i, top panel) and N-doped graphene (ii, bottom panel) from undoped and highly N-doped SiC substrate ($n = 7.4 \times 10^{18}$ cm$^{-3}$), respectively, to characterize their atomic composition and chemical bonding. The solid and dotted lines indicate the experimental data and the sum of the curve-fitted components, respectively. The C 1s spectrum of pristine graphene can be primarily characterized by three major peaks: a carbon−carbon peak at 284.6 eV corresponding to C═C in aromatic rings indicating sp$^2$ carbon bonding; shoulder peaks at 283.8 and 285.5 eV corresponding to Si−C, and buffer layer that is carbon-rich layer between graphene and SiC substrate.[31,39] The C 1s spectrum of N-doped graphene can be mainly characterized by four peaks at C═C, Si−C, buffer layer, and C−N bonds, respectively, showing a broader spectrum range compared to the pristine graphene. The small peak at 286.5 eV indicates the binding energy corresponding to either sp$^2$-C or sp$^3$-C with nitrogen atoms.[16] In clear comparison with the pristine graphene, fwhm at 284.6 eV of the N-doped graphene increases from 1.0 to 1.24 due to the doping effect.[16,18] These results from the XPS C 1s spectra verify that N-doped graphene was successfully synthesized by laser irradiation.

Figure 2b demonstrates N 1s spectra of pristine (no signal) and N-doped graphene. Typically, for N-doped graphene, three components of C−N bonding correspond to pyridinic-N (nitrogen bonded to two carbons, 398.1−399.3 eV), pyrrolic-N (nitrogen included in pentagon ring, 399.8−401 eV), and graphitic-N (nitrogen bonded to three carbons, 401.1−402.7 eV).[7,11,16,32] Therefore, the N 1s peak located at 398.5 eV as shown in Figure 2b (ii, bottom panel) corresponds to pyridinic-N bonding. To manifest supply of nitrogen atoms from the substrate, XPS analysis was also conducted on the bare substrate prior to laser irradiation. Figure S3 in the Supporting Information shows XPS spectra on the

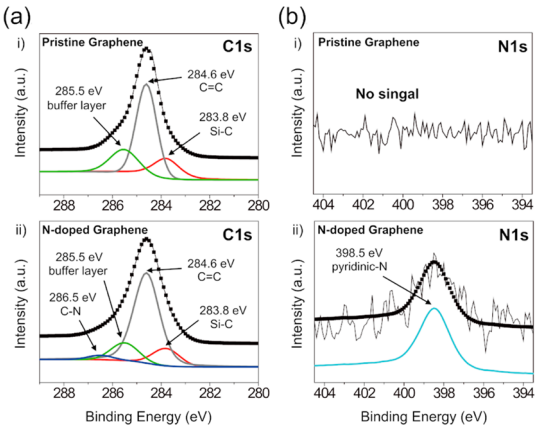


**Figure 2. XPS C 1s (a) and N 1s (b) spectra taken from pristine (i, top panel) and N-doped graphene (ii, bottom panel). The C 1s peak of pristine graphene is characterized by three peaks at 283.8, 284.6, and 285.5 eV, corresponding to Si−C, C═C, and the buffer layer, respectively. The C 1s peak of N-doped graphene is broader and decomposed into one more binding energy of 286.5 eV, corresponding to C−N bonding. The N 1s peak of N-doped graphene describes pyridinic-N bonding.**

highly N-doped SiC substrate. Compared to the N 1s spectrum of N-doped graphene, the binding energy of 397.7 eV describes Si−N−C composition. Velez-Fort *et al.* reported a method to grow *in situ* N-doped EG on 4H-SiC by exposing the substrate to nitrogen gas during the graphene growth.[16] In addition to nitrogen atoms incorporated in the graphene lattice, such as pyridinic, pyrrolic, and graphitic configurations, the presence of defects such as dangling bonds in the buffer layer facilitates the incorporation of the nitrogen atoms through formation of Si−N−C bonds. They assigned the binding energy of 397.7 eV to Si−N−C chemical states, showing a good agreement with our N 1s peak position from the substrate. The atomic concentration of nitrogen on the highly N-doped substrate was ~0.7%, while the nitrogen concentration was reduced to ~0.6% in the graphene lattice, as determined by XPS. This means that nitrogen atoms were marginally evaporated at the same time with sublimation of Si atoms by laser irradiation. Therefore, the XPS results indicate that the solid dopant sources of SiC substrate could be incorporated in the graphene lattice.

Figure 3a shows the Raman spectra of N-doped graphene on N-doped 4H-SiC produced by varying fluence with a step change of approximately 7% using a controllable energy attenuator. The characteristic 2D band of graphene is not observed at the low fluence of 1045 mJ/cm$^2$ (red line) because most of the thermal energy is diffusing into the SiC substrate due to its high thermal conductivity.[35] The G and 2D bands are clearly visible at the fluences of 1124 (green line) and 1196 mJ/cm$^2$ (blue line), respectively. However, a decay of the 2D band with an increase of the D band is remarkably observed at the high fluence of 1301 mJ/cm$^2$ (cyan line).

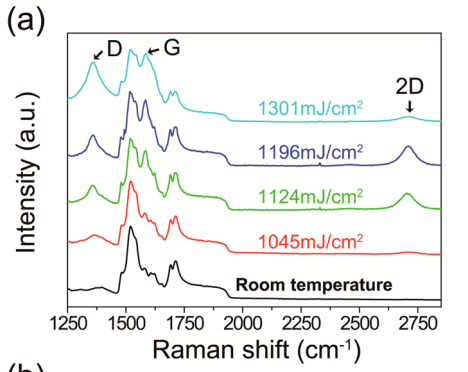


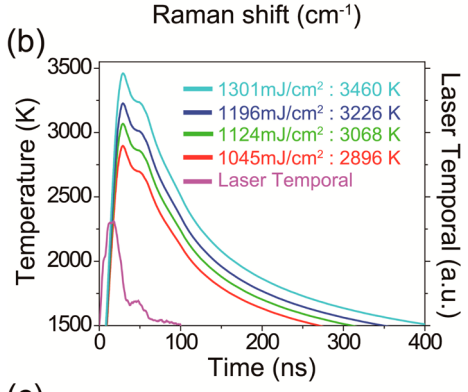


(c)

| Laser fluence (mJ/cm²) | 1045 | 1124 | 1196 | 1301 |
|---|---|---|---|---|
| Simulated maximum temperature (K) | 2896 | 3068 | 3226 | 3460 |
| Raman analysis | x | D,G,2D | D,G,2D | D,G |

**Figure 3. (a) Raman spectra on the SiC surface corresponding to various laser fluences of 1045 mJ/cm$^2$ (red line), 1124 mJ/cm$^2$ (green line), 1196 mJ/cm$^2$ (blue line), and 1301 mJ/cm$^2$ (cyan line). The black line shows the characteristic of 4H-SiC. (b) Simulated temperature distribution as a function of time using single pulse. The maximum surface temperatures correspond to 2896 K at 1045 mJ/cm$^2$ (red line), 3068 K at 1124 mJ/cm$^2$ (green line), 3226 K at 1196 mJ/cm$^2$ (blue line), and 3460 K at 1301 mJ/cm$^2$ (cyan line). Violet line shows laser temporal data. (c) The simulated maximum surface temperatures and Raman results on the SiC surface corresponding to laser fluences such as 1045, 1124, 1196, and 1301 mJ/cm$^2$.**

In order to understand the growth temperature for N-doped graphene corresponding to laser fluence (*i.e.*, thermal energy), a numerical simulation was performed with reference to the previous articles of Im and Fogarassy.[24−27] Figure 3b presents a numerical simulation of thermal behavior (*i.e.*, heat generation and cooling) corresponding to various fluence conditions. Thermal and optical parameters used in this simulation are described in the Methods.[40,41] The simulated maximum surface temperatures resulting from a single pulse (violet line) are 2896 K at 1045 mJ/cm$^2$ (red line), 3068 K at 1124 mJ/cm$^2$ (green line), 3226 K at 1196 mJ/cm$^2$ (blue line), and 3460 K at 1301 mJ/cm$^2$ (cyan line), respectively. Figure S4 in the Supporting Information indicates the simulated temperature distribution in the vertical direction from the SiC surface to bulk. Only hundreds of nanometers from the top surface are influenced by the high thermal energy of the laser irradiation. Although one pulse can deposit high thermal energy on the SiC surface, we experimentally confirmed in the Raman spectra that hundreds of irradiations are required to form the graphene lattice, owing to the short pulse duration.[20,21]

The simulated maximum surface temperature and Raman results corresponding to laser fluences are summarized in Figure 3c. The N-doped graphene was successfully synthesized with fluences of 1124 and 1196 mJ/cm$^2$, while no graphitized carbon was observed at the low fluence of 1045 mJ/cm$^2$. On the other hand, a surface temperature of over 3460 K (cyan line) at 1301 mJ/cm$^2$ causes damage (*i.e.*, ablation of carbon) on the SiC surface. From the experimental and simulation results, we propose both the proper thermal energy (*i.e.*, 1124 or 1196 mJ/cm$^2$) and the number of irradiations (*i.e.*, 600 pulses) that are required to synthesize graphene on SiC by pulsed laser irradiation.

Intensive studies of doped graphene grown by CVD method have presented the G band shift as a fingerprint of doping since the incorporation of heteroatoms breaks the symmetry of the graphene lattice.[32−34] We carried out a systematic Raman analysis of N-doped graphene grown on a hexagonal SiC surface with different dopant concentrations (Figure 4). In this work, we used four different substrates: undoped ($n < 1 \times 10^{16}$ cm$^{-3}$) 6H-SiC, low-doped ($n = 9 \times 10^{17}$ cm$^{-3}$) 6H-SiC, mid-doped ($n = 2.2 \times 10^{18}$ cm$^{-3}$) 4H-SiC, and high-doped ($n = 7.4 \times 10^{18}$ cm$^{-3}$) 4H-SiC. By utilizing a micro-Raman system with 514.5 nm excitation, we investigated all the samples over the same positions (*i.e.*, central areas of the samples). The average values of the G band position represented by star labels were blueshifted with respect to the dopant concentrations of four different substrates. The G band position of the pristine graphene exhibits between 1581 and 1582.5 cm$^{-1}$, whereas N-doped graphene grown on the low-doped 6H-SiC presents a slight blueshift between 1582.5 and 1584 cm$^{-1}$. Figure S5 in the Supporting Information shows the representative Raman spectra of the pristine and the N-doped graphene.

In order to investigate the relationship between the G band shift and the dopant concentration of SiC, we systematically studied the G band positions of N-doped graphene from mid-doped ($n = 2.2 \times 10^{18}$ cm$^{-3}$) and high-doped ($n = 7.4 \times 10^{18}$ cm$^{-3}$) 4H-SiC. The G band position of N-doped graphene grown on the high-doped 4H-SiC shows a noticeable blueshift compared to results on the mid-doped 4H-SiC. This shift originates from an increased structural disorder due to the disruptions in the sp$^2$ carbon honeycomb lattice by the incorporation of nitrogen atoms.[42] In addition, we examined the characteristic feature of the laser-induced graphene grown on both Si and C faces. The systematic analysis of pristine and N-doped graphene (*i.e.*, grown on low-doped SiC) confirms that G band peaks of graphene grown from

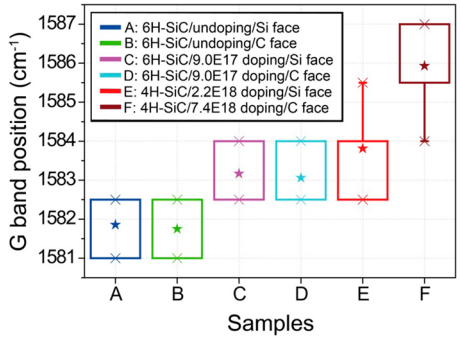


**Figure 4. Systematic analysis on the G band position of the graphene grown on the SiC with different dopant concentration: undoped ($n < 1 \times 10^{16}$ cm$^{-3}$) 6H-SiC, low-doped ($n = 9 \times 10^{17}$ cm$^{-3}$) 6H-SiC, mid-doped ($n = 2.2 \times 10^{18}$ cm$^{-3}$) 4H-SiC, and high-doped ($n = 7.4 \times 10^{18}$ cm$^{-3}$) 4H-SiC. Star labels represent the average value of the G band positions from each substrate. X marks indicate minimum and maximum position from each substrate.**

Si and C faces appear at the same position. Therefore, the position of the G band is dominantly shifted by the dopant concentration of the SiC substrate. More details of this characteristic from the investigation on the G band positions are shown in Supporting Information, Figure S6.

The SiC-derived graphene layers could be under a compressive strain that leads to a blueshift of G band.[43] The thermally grown EG on the Si-terminated surface of SiC is governed by the formation of the $(6\sqrt{3} \times 6\sqrt{3})$ $R30°$ reconstruction, which acts as an intermediate phase of graphitization.[39] It consists of an initial carbon rich layer in a graphene-like honeycomb arrangement with approximately 30% of the carbon atoms which are covalently bonding down to the Si atoms of the substrate. Hence, this layer is electronically coupled with substrate and called "0th layer" or "buffer layer". Increasing the temperature higher than the formation of the carbon-rich buffer layer leads to creation of the first graphene layer on the buffer layer and compressive strain forms due to the different thermal expansion coefficients between graphene and SiC during the cooling down from the growth temperature.

On the other hand, Lee *et al*. proved no periodic surface reconstruction of the laser-synthesized graphene through close investigation using synchrotron-based X-ray diffraction and scanning tunneling microscopy.[20] Furthermore, the 2D peak of the laser-induced multilayer graphene on Si-terminated surface of SiC was in a good harmony with single Lorentzian. Single-peak fitting of the 2D peak normally observed in multilayer EG on the C-terminated surface of SiC by thermal decomposition in furnace, providing a sign of electronic decoupling between the graphene layers. Therefore, their Raman analysis suggests that the laser-synthesized multilayer graphene on Si-terminated surface of SiC are not Bernal-stacked and electronically decoupled. This means no strong compressive strain could be generated from the substrate, but possibly a weak coupling arises. Recently, our group found a new metastable phase transition of amorphous layer on a hexagonal SiC surface as an intermediate phase of graphitization on both Si and C faces rather than surface reconstruction, which might be only discovered by short pulse laser irradiation. From the experimental results of Lee and our group, laser-induced graphene on SiC substrate has a different interface layer and growth mechanism, compared to thermally grown EG, due to extremely short heat deposition of 30 ns.

In addition, Ferralis *et al*. reported that a blueshift of the G band by compressive strain monotonically increases as the annealing time prolongs, such as several tens of minutes.[44] In the case of pulse laser irradiation, we showed that heat deposition of 1 pulse was ~30 ns and completely cooled down under 1 $\mu$s in the simulated temperature data, as shown in the Figure 3b. Therefore, from the analysis results, we exclude an effect of compressive strain from the substrate regarding to G band shift because laser-induced graphene has different condition of interface layer compared to thermally grown EG.

## CONCLUSIONS

In summary, we report a novel synthesis of laser-induced N-doped graphene on hexagonal SiC which includes a solid dopant source. This method provides the direct growth of doped graphene on an insulating substrate without an additional transfer procedure. The XPS analysis confirms that the C—N bonding conformation of the N-doped graphene was pyridinic-N type. Systematic analysis of the G band shift in the Raman spectra suggests that solid-phase doping can provide precise controllability of doping concentration by simply changing the dopant concentration of SiC. Furthermore, the G band shift depends dominantly on the dopant concentration of the SiC substrate. Simulated temperature history indicates that heat generation on the SiC by short pulse of laser irradiation is high enough to synthesize N-doped graphene. We are currently exploring the new intermediate phase of laser-induced N-doped graphene on SiC to clarify the growth mechanism by extremely short heat deposition. This work is expected to provide a solid-phase doping strategy with excellent controllability, which is primarily used in advanced Si CMOS technology.

## METHODS

**Sample Preparation for Laser Irradiation.** To synthesize pristine and N-doped graphene, undoped ($n < 1 \times 10^{16}$ cm$^{-3}$) and low-doped ($n = 9 \times 10^{17}$ cm$^{-3}$) 6H-SiC (0001) wafers with chemical mechanical polishing (CMP, RMS ≤ 1 nm) were prepared and supplied by Prof. Won Jae Lee's group from

Dong-Eui University. Mid-doped ($n = 2.2 \times 10^{18}$ cm$^{-3}$) and high-doped ($n = 7.4 \times 10^{18}$ cm$^{-3}$) 4H-SiC wafers with CMP were purchased from Cree. These specimens, sized 8 mm × 8 mm, were cut from the wafers and cleaned by sequential ultrasonic baths in acetone, isopropyl alcohol, and deionized water to remove grease. Pirana solution (mixture of $H_2SO_4/H_2O_2$ = 3:1) and BOE etchant (10:1) were used for 3 min to completely remove organic contamination and surface oxide, respectively.[20,21] After the cleaning process, each SiC substrate was placed in a vacuum chamber (Linkam, TS1000) and heated to 600 °C for 1 h under low vacuum conditions (~$3.0 \times 10^{-3}$ Torr) to remove surface contamination such as adsorbed oxygen. The substrate temperature was maintained at 600 °C, which is irrelevant to growth condition of graphene, during laser irradiation.

**Characterization: Raman/XPS/TEM.** Micro-Raman measurements with a spot size of about 1 $\mu$m were performed at room temperature with LabRAM Aramis (Horiba Jobin Yvon) using Ar ion laser (514.5 nm) focused on pristine and N-doped graphene by optical microscope with a 50× objective lens. XPS analysis was carried out using a microfocused monochromatic Al Kα excitation with a base pressure of $5 \times 10^{-9}$ Torr (Sigma Probe, Thermo VG Scientific, Inc.). Cross-sectional TEM samples were prepared using a focused ion beam (FIB, FEI Quanta 3D) lift out technique. Prior to Ga-ion milling, the samples were protected with amorphous carbon coating as a capping layer to preserve the initial surface integrity. The HRTEM images were taken with JEOL JEM 2100F with a probe Cs corrector at 200 kV.

**Numerical Simulation.** The numerical simulation performed in the present study is widely used for the analysis of thermal behavior regarding laser-solid interaction involving heat generation and cooling at the surface of the irradiated area by light absorption.[24−27] Thermal simulation parameters of SiC were referenced to Nilsson's article and modified to $\{720/(T - 69)\}$ of thermal conductivity and $\{1.12 \ln (T) - 4\}$ of heat capacity as a function of high temperature, respectively.[41] In addition, the reflective index *n* and *k* as optical parameters were set to 2.9 and 0.1 at 308 nm.[40] Temporal data of our 308 nm XeCl laser, as shown in Figure S2 (Supporting Information), and optimized experimental conditions (*i.e.*, fluence and substrate heating) were used to investigate temperature history on the N-doped SiC during short pulse duration (30 ns).

*Conflict of Interest:* The authors declare no competing financial interest.

*Acknowledgment.* We acknowledge financial support from the Basic Science Research Program (NRF-2012R1A2A1A03010415, CAFDC/K. J. Lee/No. 2013042126), the Nano·Material Technology Development Program (2012M3A7B4049807), and the Creative Research Program of ETRI (13ZE1110), Korea. We thank Dukin Co., Ltd., for their support of the laser system (SLS-200), Dr. Jeongwon Kim and Mr. Tae Gun Kim at KRISS for help with the XPS analysis, and Dr. A. B. Limanov and Prof. J. S. Im at Columbia University for their valuable discussion and comments related to the simulation.

*Supporting Information Available:* Details of 308 nm XeCl excimer laser system (Figure S1), temporal data of 308 nm XeCl excimer laser (Figure S2), XPS analysis on highly N-doped SiC substrate (Figure S3), temperature distribution in the vertical direction from the SiC surface to bulk (Figure S4), Raman spectra of pristine and N-doped graphene (Figure S5), and systematic analysis of G band position on various substrates (Figure S6). This material is available free of charge *via* the Internet at http://pubs.acs.org.

## REFERENCES AND NOTES

1. Geim, A. K.; Novoselov, K. S. The Rise of Graphene. *Nat. Mater.* **2007**, *6*, 183–191.
2. Katsnelson, M. I.; Novoselov, K. S. Graphene: New Bridge between Condensed Matter Physics and Quantum Electrodynamics. *Solid State Commun.* **2007**, *143*, 3–13.
3. Morozov, S. V.; Novoselov, K. S.; Katsnelson, M. I.; Schedin, F.; Elias, D. C.; Jaszczak, J. A.; Geim, A. K. Giant Intrinsic Carrier Mobilities in Graphene and Its Bilayer. *Phys. Rev. Lett.* **2008**, *100*, 016602.
4. Kim, K.; Choi, J. Y.; Kim, T.; Cho, S. H.; Chung, H. J. A Role for Graphene in Silicon-Based Semiconductor Devices. *Nature* **2011**, *479*, 338–344.
5. Schwierz, F. Graphene Transistors. *Nat. Nanotechnol.* **2010**, *5*, 487–496.
6. Liu, H. T.; Liu, Y. Q.; Zhu, D. B. Chemical Doping of Graphene. *J. Mater. Chem.* **2011**, *21*, 3335–3345.
7. Wang, H. B.; Maiyalagan, T.; Wang, X. Review on Recent Progress in Nitrogen-Doped Graphene: Synthesis, Characterization, and Its Potential Applications. *ACS Catal.* **2012**, *2*, 781–794.
8. Wei, D. C.; Liu, Y. Q.; Wang, Y.; Zhang, H. L.; Huang, L. P.; Yu, G. Synthesis of N-Doped Graphene by Chemical Vapor Deposition and Its Electrical Properties. *Nano Lett.* **2009**, *9*, 1752–1758.
9. Jin, Z.; Yao, J.; Kittrell, C.; Tour, J. M. Large-Scale Growth and Characterizations of Nitrogen-Doped Monolayer Graphene Sheets. *ACS Nano* **2011**, *5*, 4112–4117.
10. Zhao, L. Y.; He, R.; Rim, K. T.; Schiros, T.; Kim, K. S.; Zhou, H.; Gutierrez, C.; Chockalingam, S. P.; Arguello, C. J.; Palova, L.; et al. Visualizing Individual Nitrogen Dopants in Monolayer Graphene. *Science* **2011**, *333*, 999–1003.
11. Usachov, D.; Vilkov, O.; Gruneis, A.; Haberer, D.; Fedorov, A.; Adamchuk, V. K.; Preobrajenski, A. B.; Dudin, P.; Barinov, A.; Oehzelt, M.; et al. Nitrogen-Doped Graphene: Efficient Growth, Structure, and Electronic Properties. *Nano Lett.* **2011**, *11*, 5401–5407.
12. Zhang, C. H.; Fu, L.; Liu, N.; Liu, M. H.; Wang, Y. Y.; Liu, Z. F. Synthesis of Nitrogen-Doped Graphene Using Embedded Carbon and Nitrogen Sources. *Adv. Mater.* **2011**, *23*, 1020–1024.
13. Kim, K. S.; Zhao, Y.; Jang, H.; Lee, S. Y.; Kim, J. M.; Kim, K. S.; Ahn, J. H.; Kim, P.; Choi, J. Y.; Hong, B. H. Large-Scale Pattern Growth of Graphene Films for Stretchable Transparent Electrodes. *Nature* **2009**, *457*, 706–710.
14. Bae, S.; Kim, H.; Lee, Y.; Xu, X. F.; Park, J. S.; Zheng, Y.; Balakrishnan, J.; Lei, T.; Kim, H. R.; Song, Y. I.; et al. Roll-to-Roll Production of 30-Inch Graphene Films for Transparent Electrodes. *Nat. Nanotechnol.* **2010**, *5*, 574–578.
15. Song, J.; Kam, F. Y.; Png, R. Q.; Seah, W. L.; Zhuo, J. M.; Lim, G. K.; Ho, P. K. H.; Chua, L. L. A General Method for Transferring Graphene onto Soft Surfaces. *Nat. Nanotechnol.* **2013**, *8*, 356–362.
16. Velez-Fort, E.; Mathieu, C.; Pallecchi, E.; Pigneur, M.; Silly, M. G.; Belkhou, R.; Marangolo, M.; Shukla, A.; Sirotti, F.; Ouerghi, A. Epitaxial Graphene on 4H-SiC(0001) Grown under Nitrogen Flux: Evidence of Low Nitrogen Doping and High Charge Transfer. *ACS Nano* **2012**, *6*, 10893–10900.
17. Wang, Z. J.; Wei, M. M.; Jin, L.; Ning, Y. X.; Yu, L.; Fu, Q.; Bao, X. H. Simultaneous N-Intercalation and N-Doping of Epitaxial Graphene on 6H-SiC(0001) through Thermal Reactions with Ammonia. *Nano Res.* **2013**, *6*, 399–408.
18. Velez-Fort, E.; Pallecchi, E.; Silly, M. G.; Bahri, M.; Patriarche, G.; Shukla, A.; Sirotti, F.; Ouerghi, A. Single Step Fabrication of N-doped Graphene/$Si_3N_4$/SiC Heterostructures. *Nano Res.* **2014**, *7*, 835–843.
19. Telychko, M.; Mutombo, P.; Ondracek, M.; Hapala, P.; Bocquet, F. C.; Kolorenc, J.; Vondracek, M.; Jelinek, P.; Svec, M., Achieving High-Quality Single-Atom Nitrogen Doping of Graphene/SiC(0001) by Ion Implantation and Subsequent Thermal Stabilization. *ACS Nano* DOI: 10.1021/nn502438k.
20. Lee, S.; Toney, M. F.; Ko, W.; Randel, J. C.; Jung, H. J.; Munakata, K.; Lu, J.; Geballe, T. H.; Beasley, M. R.; Sinclair, R.; et al. Laser-Synthesized Epitaxial Graphene. *ACS Nano* **2010**, *4*, 7524–7530.
21. Hwang, H. J.; Cho, C.; Lim, S. K.; Lee, S. Y.; Kang, C. G.; Hwang, H.; Lee, B. H. Electrical Characteristics of Wrinkle-Free Graphene Formed by Laser Graphitization of 4H-SiC. *Appl. Phys. Lett.* **2011**, *99*, 082111.
22. Kim, T. I.; Jung, Y. H.; Song, J. Z.; Kim, D.; Li, Y. H.; Kim, H. S.; Song, I. S.; Wierer, J. J.; Pao, H. A.; Huang, Y. G.; et al. High-Efficiency, Microscale GaN Light-Emitting Diodes and Their Thermal Properties on Unusual Substrates. *Small* **2012**, *8*, 1643–1649.

23. Kim, Y. H.; Sohn, C. Y.; Lim, J. W.; Yun, S. J.; Hwang, C. S.; Chung, C. H.; Ko, Y. W.; Lee, J. H. High-Performance Ultralow-Temperature Polycrystalline Silicon TFT Using Sequential Lateral Solidification. *IEEE Electron Device Lett.* **2004**, *25*, 550–552.
24. Gupta, V. V.; Song, H. J.; Im, J. S. Numerical Analysis of Excimer-Laser-Induced Melting and Solidification of Thin Si Films. *Appl. Phys. Lett.* **1997**, *71*, 99–101.
25. Leonard, J. P.; Im, J. S. Modelling Solid Nucleation and Growth in Supercooled Liquid. *Mater. Res. Soc. Symp. Proc.* **1999**, *580*, 233–244.
26. Leonard, J. P.; Im, J. S. Stochastic Modeling of Solid Nucleation in Supercooled Liquids. *Appl. Phys. Lett.* **2001**, *78*, 3454–3456.
27. Dutto, C.; Fogarassy, E.; Mathiot, D. Numerical and Experimental Analysis of Pulsed Excimer Laser Processing of Silicon Carbide. *Appl. Surf. Sci.* **2001**, *184*, 362–366.
28. Scace, R. I.; Slack, G. A. Solubility of Carbon in Silicon and Germanium. *J. Chem. Phys.* **1959**, *30*, 1551–1555.
29. Berger, C.; Song, Z. M.; Li, T. B.; Li, X. B.; Ogbazghi, A. Y.; Feng, R.; Dai, Z. T.; Marchenkov, A. N.; Conrad, E. H.; First, P. N.; et al. Ultrathin Epitaxial Graphite: 2D Electron Gas Properties and a Route toward graphene-based nanoelectronics. *J. Phys. Chem. B* **2004**, *108*, 19912–19916.
30. Berger, C.; Song, Z. M.; Li, X. B.; Wu, X. S.; Brown, N.; Naud, C.; Mayou, D.; Li, T. B.; Hass, J.; Marchenkov, A. N.; et al. Electronic Confinement and Coherence in Patterned Epitaxial Graphene. *Science* **2006**, *312*, 1191–1196.
31. Emtsev, K. V.; Bostwick, A.; Horn, K.; Jobst, J.; Kellogg, G. L.; Ley, L.; McChesney, J. L.; Ohta, T.; Reshanov, S. A.; Rohrl, J.; et al. Towards Wafer-Size Graphene Layers by Atmospheric Pressure Graphitization of Silicon Carbide. *Nat. Mater.* **2009**, *8*, 203–207.
32. Zafar, Z.; Ni, Z. H.; Wu, X.; Shi, Z. X.; Nan, H. Y.; Bai, J.; Sun, L. T. Evolution of Raman Spectra in Nitrogen Doped Graphene. *Carbon* **2013**, *61*, 57–62.
33. Panchokarla, L. S.; Subrahmanyam, K. S.; Saha, S. K.; Govindaraj, A.; Krishnamurthy, H. R.; Waghmare, U. V.; Rao, C. N. R. Synthesis, Structure, and Properties of Boron- and Nitrogen-Doped Graphene. *Adv. Mater.* **2009**, *21*, 4726–4730.
34. Stampfer, C.; Molitor, F.; Graf, D.; Ensslin, K.; Jungen, A.; Hierold, C.; Wirtz, L. Raman Imaging of Doping Domains in Graphene on $SiO_2$. *Appl. Phys. Lett.* **2007**, *91*, 241907.
35. Pensl, G.; Ciobanu, F.; Frank, T.; Krieger, M.; Reshanov, S.; Schmid, F.; Weidner, M. SiC Material Properties. *Int. J. High Speed Electron. Syst.* **2005**, *15*, 705745.
36. Ferrari, A. C. Raman Spectroscopy of Graphene and Graphite: Disorder, Electron-Phonon Coupling, Doping and Nonadiabatic Effects. *Solid State Commun.* **2007**, *143*, 47–57.
37. Ni, Z. H.; Chen, W.; Fan, X. F.; Kuo, J. L.; Yu, T.; Wee, A. T. S.; Shen, Z. X. Raman Spectroscopy of Epitaxial Graphene on a SiC Substrate. *Phys. Rev. B* **2008**, *77*, 115416.
38. Yannopoulos, S. N.; Siokou, A.; Nasikas, N. K.; Dracopoulos, V.; Ravani, F.; Papatheodorou, G. N. $CO_2$-Laser-Induced Growth of Epitaxial Graphene on 6H-SiC(0001). *Adv. Funct. Mater.* **2012**, *22*, 113–120.
39. Riedl, C.; Coletti, C.; Starke, U. Structural and Electronic Properties of Epitaxial Graphene on SiC(0001): A Review of Growth, Characterization, Transfer Doping and Hydrogen Intercalation. *J. Phys. D: Appl. Phys.* **2010**, *43*, 374009.
40. Pegourie, B. Optical-Properties of Alpha-Silicon Carbide. *Astron. Astrophys.* **1988**, *194*, 335–339.
41. Nilsson, O.; Mehling, H.; Horn, R.; Fricke, J.; Hofmann, R.; Muller, S. G.; Eckstein, R.; Hofmann, D. Determination of the Thermal Diffusivity and Conductivity of Mono Crystalline Silicon Caride (300−2300 K). *High Temp.-High Pressures* **1997**, *29*, 73–79.
42. Lin, Y. C.; Lin, C. Y.; Chiu, P. W. Controllable Graphene N-Doping with Ammonia Plasma. *Appl. Phys. Lett.* **2010**, *96*, 133110.
43. Rohrl, J.; Hundhausen, M.; Emtsev, K. V.; Seyller, T.; Graupner, R.; Ley, L. Raman Spectra of Epitaxial Graphene on SiC(0001). *Appl. Phys. Lett.* **2008**, *92*, 201918.
44. Ferralis, N.; Maboudian, R.; Carraro, C. Evidence of Structural Strain in Epitaxial Graphene Layers on 6H-SiC(0001). *Phys. Rev. Lett.* **2008**, *101*, 156801.